Surface characterization of poly(acrylonitrile) based intermediate modulus carbon fibres

M. DESAEGER, M. J. REIS*, A. M. BOTELHO do REGO*, J. D. LOPES da SILVA*, I. VERPOEST
Katholieke Universiteit Leuven, MTM, de Croylaan 2, 3001 Heverlee, Belgium
* Centro de Química-Física Molecular, Complexo I, IST, 1096 Lisboa Codex, Portugal

The interface between the fibre and the matrix is a very important factor influencing the mechanical behaviour of composite materials. For superior composite performance, one must not only select optimal fibres and matrices, but also optimize the interface between them. However, the control of the interface properties is not an easy task. This work is an interdisciplinary and integrated approach to the problem. The effect of different degrees of a wet oxidative surface treatment on the surface of poly(acrylonitrile) based intermediate modulus carbon fibres (Courtaulds IM CG43-750) has been studied using classical thermodynamic as well as spectroscopic techniques, aimed at obtaining a complete physical and chemical characterization of the fibre surface. The results show that all aspects of the fibre surface are influenced by the surface treatments, which are specially designed to improve the adhesion between fibre and matrix. The study outlines the most important surface features improving this adhesion. The results concerning the characterization of the fibre surface contribute, when combined with micromechanical tests, to clarifying the adhesion mechanisms, revealing, at the same time, a mechanical interlocking and a chemical interaction.

1. Introduction

Commercial carbon fibres are usually obtained from poly(acrylonitrile) (PAN) precursor fibres by a stabilization and carbonization treatment, and a final heat treatment at high temperature. Based on the carbonization temperature, the carbon fibres are grouped according to their structure and degree of crystallite orientation. High-modulus (HM) fibres are obtained from the uppermost carbonization temperatures (> 2000 °C), while high-strength (HS) fibres have a carbonization temperature between 1000–1600 °C. A recent development is the IM-fibre (intermediate modulus), a fibre with the strength of HS fibres, but with improved modulus values.

HS and HM fibres have already received a lot of attention and general models for their microstructure are generally accepted. Since the IM fibres were developed later, they are less known and no general description of their microstructure is available. Nevertheless, the high modulus of these fibres makes an entire characterization of its surface worthwhile [1, 2].

It is well known that the adhesion between carbon fibres and an epoxy matrix is intrinsically very poor. This is why different kinds of surface treatments were developed and applied to the fibres at the end of the production line in order to improve the mechanical performance of composites based on carbon fibres [3, 4]. Several methods have been tried to modify the

fibre surface, though most of them are based on the application of oxidative surface treatments.

The increase of the adhesion between the surface-treated carbon fibre and the polymer matrix may be explained by the fact that various physical and chemical changes are induced at the fibre surface after surface treatments [5]. In the present work, the effects induced by several degrees of an oxidative surface treatment on PAN-based intermediate-modulus carbon fibres have been studied, using several techniques. It is the first time that such a variety of surface characterization techniques have been applied to the same fibres, giving compatible and complementary results.

For the topography characterization, techniques like scanning electron microscopy (SEM) which gives a general view concerning the morphology of the fibre surface, as well as gas adsorption techniques, that allow the determination of the total surface area (TSA) and the microporosity of the fibres, were used. The chemical state of the fibre surface was characterized by oxygen chemisorption techniques, determining the activated surface area (ASA), and by X-ray photoelectron spectroscopy [6–9]. Other thermodynamic properties such as surface energy, its polar and dispersive components, have provided useful and complementary information; the contact angle method was used for surface energy measurements [10].

2. Experimental procedure

Experiments were performed on four commercial IM carbon fibres (Courtaulds (CG43-750, tensile strength 5.5 GPa, tensile Young's modulus 310 GPa) which have undergone the same oxidative surface treatment but at various levels: 0, 10, 50 and 100% STL surface treatment level); 0% is the untreated fibre and 100% the full commercially treated fibre. The exact nature and conditions of the surface treatment are proprietary and can not be published. In the following we will refer separately to the used techniques.

2.1. Gas adsorption measurements

For these measurements two methods have been used: a volumetric method with krypton and a gravimetric method with nitrogen.

In the volumetric method, measurements were carried out with an ASAP2000 from Micromeritics. Samples have been degassed at two different temperatures, room temperature (RT) and 130 °C, under a vacuum of 4×10^{-2} Pa for 1 h. The sample was then submitted to five different relative pressures of krypton. The amount of adsorbed gas was monitored and the Brauner–Emmett–Teller (BET) model was applied to derive the specific surface area of the fibre.

In the gravimetric method, samples have been degassed under a vacuum of 1×10^{-2} Pa for 24 h at RT and 130 °C. The adsorption apparatus included a Cahn RG100 microbalance connected to a gas vacuum line where nitrogen could be dosed at variable pressures in the range of 1–101 kPa. The adsorption occurred at 77 K. Full adsorption–desorption isotherms were obtained and the BET model was also applied for the determination of the fibre specific surface area using a molecular area of 0.162 nm^2 for nitrogen. Microporosity was assessed from the difference between the two isotherms (RT and 130 °C). By heating the fibre, the water entrapped in the micropore is removed and hence the microporosity, expressed in μmoles N_2 per gram fibre, can be measured.

2.2. Oxygen chemisorption

Oxygen chemisorption measurements were made gravimetrically on the same apparatus used for the determination of the specific surface area with nitrogen. Samples were submitted to a pretreatment at 950 °C under a vacuum of 4×10^{-2} Pa (in these conditions, it is assumed that all the oxygen present at the fibre surface is released) followed by oxygen chemisorption at 340 °C, leading to the formation of carbonyl groups on the active sites present at the fibre surface. The total amount of adsorbed oxygen was monitored and the number of active sites determined by multiplying by a factor 2 the number of molecules of O_2 dissociatively adsorbed. The active surface area was determined assuming that the area of each oxygen atom is 0.083 nm^2.

2.3. X-ray photoelectron spectroscopy

Samples were analysed by X-ray photoelectron spec-troscopy (XPS) using a XSAM800 (Kratos) X-ray Spectrometer (Lab 1 – CQFM, Lisbon) operated in the FAT mode, with a pass energy of 10 eV with the non-monochromatized Mg X-radiation ($hv = 1253.7$ eV). The base pressure in the sample chamber was in the range of 10^{-7} Pa. Fibre samples were mounted in a bundle arrangement such that no part of the sample probe could be detected during data acquisition. All the sample transfers were made in air.

All fibres were analysed at room temperature, without further treatment, at a take-off angle (TOA) of 90°. In order to check for the presence of traces of the oxidative treatment bath, two tests have been performed. The exact nature and conditions of the surface treatment are proprietary and can not be published. However, if some traces were present, gaseous nitrogen would evolve by heating. In the first test, 100% STL fibre was analysed after being boiled for 30 min, air dried at 130 °C and kept under ultra-high vaccum (UHV) for 2 months (due to a break down of the XPS acquisition system). After a first run at these conditions, a second test was performed on the same fibre, further heated to 250 °C for 30 min and analysed once more.

Spectra were collected and stored in 200 channels with a step of 0.1 eV using a PDP-11/73 microcomputer from Scientific Micro Systems, Inc. using DS800 software, from Kratos, for spectral acquisition, storage and processing. The curve fitting was carried out with a nonlinear least-squares algorithm using a mixed Gaussian–Lorentzian peak shape, 85% gaussian (GL85 profile) for component peaks.

Some of the results have been cross checked with results obtained using two other spectrometers: Lab 2 (LISE, Namur), used a Hewlett Packard 5950A, equipped with an X-ray monochromator, which gives a typical resolution of 0.55 eV measured as a full width at half-maximum (FWHM) of the graphite C 1s line. Its multichannel analyser is directly connected via a coupler-controller (HP2570A) to a programmable desk calculator HP9810A. All the spectra were recorded at a take-off angle of 35°. AlK_α radiation was used. In Lab 3 (University of Sheffield), the XPS spectra were obtained with the use of a VG Scientific apparatus operating at a vacuum of the order of 10^{-6} Pa, with MgK_α radiation. The electron analyser is a CLAM200 and 4 mm entrance and exit slits were used. The spectrometer was interfaced to a PDP 11/35 data system using VGS5250 software for spectral acquisition, storage and processing. Each specimen was analysed by a combination of 1000 eV survey and 20 eV high-resolution scans for all the relevant elements that could be present: carbon, oxygen and nitrogen.

2.4. Surface energy measurements

Surface energy measurements were carried out on carbon fibre single filaments using the Fowkes–Kaelble–Dann–Owens and Wendt technique,in a C. I. Electronics recording microbalance with a sensitivity of ± 1 μg, which monitors force measurements on immersion of the sample into a series of six high-purity

test liquids, thermostated at 20 °C. The liquids used were hexane, ethyleneglycol, ethanol, bromonaphthalene, water and formamide. Analysis of the contact angle measurements to yield surface energy values followed the graphical technique outlined by Kaelble [10].

3. Results and discussion
3.1. Scanning electron microscopy (SEM)
Fig. 1 shows a single typical image of an IM fibre. At this scale the surface looks smooth, the only features being longitudinal ridges over the whole length of the fibre. These ridges have already been observed on other carbon fibres and are often related to the shrinkage of the fibre during the heat treatment process [11]. The surfaces of the untreated and the treated fibres studied by SEM are similar. This reinforces the idea that the presence of the ridges is linked to the manufacturing process and not due to the application of the surface treatment.

3.2. Total surface area (TSA) and microporosity
Specific total surface areas obtained with both gravimetric and volumetric techniques for the four fibres are shown in Fig. 2. The results from the two techniques are in complete agreement and show, as a general tendency, a decrease of the total surface area of the fibre, induced by the surface treatment. The large standard deviation (SD) obtained on the results for the 10% STL fibre (SD $= 0.25$ m^2 g^{-1}) compared to the standard deviation obtained with other fibres (SD $= 0.10$ m^2 g^{-1}) shows that, at the beginning, the surface treatment causes some inhomogeneity.

BET results could lead to the conclusion that an entirely different tendency is observed when compared with results obtained by Marshall and Price [12] using scanning tunnelling microscopy (STM), for the analysis of IM fibres. The use of the STM technique shows that, after a fibre surface treatment, the homogeneous periodic waves along the fibre length and all over the fibre surface are replaced, in some regions, by more pronounced steps. It could be thought that these steps would induce an increase of the surface area. In reality, this is not the case: the specific surface area
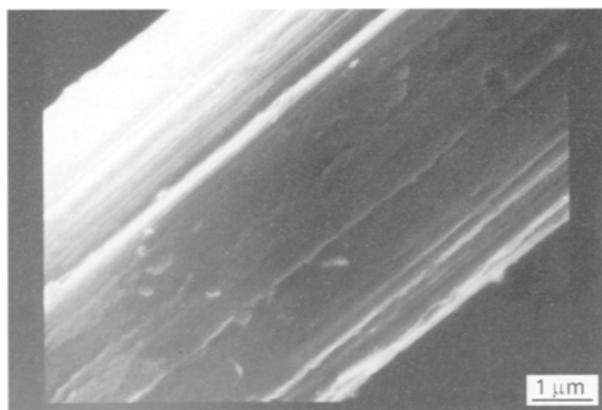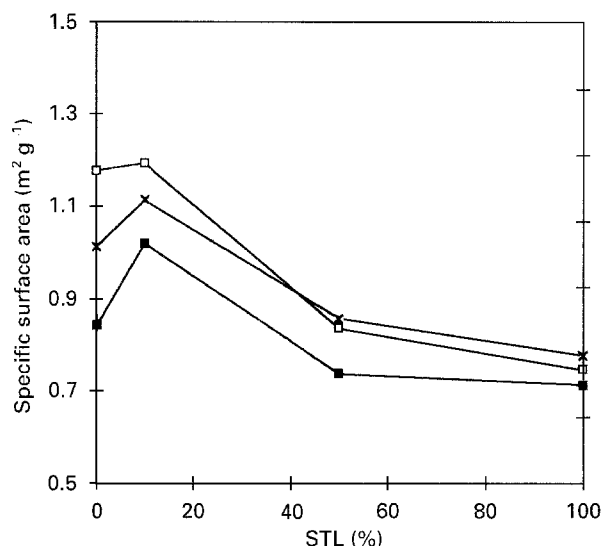

Figure 2 Surface area and microporosity as a function of STL. Key, (*) gravimetric TSA (130 °C), (□) Volumetric TSA (130 °C) and (■) microporosity.

does not increase with the surface treatment but decreases. These two apparently contradictory results can be made compatible: firstly it has to be noted that the dimensions of the steps are nearly the same as those of the periodic waves. Secondly, even if the steps start to protrude after a surface treatment of 50%, this phenomenon seems to take place only in restricted regions of the fibre whereas, in other places, the fibre seems to become smoother. Therefore, it is acceptable that, even if locally the roughness changes with the surface treatment, globally the surface treatment induces a decrease of the total surface area.

Fig. 2 also shows microporosity results. The treatment first induces an increase of microporosity, then a decrease.

3.3. Oxygen chemisorption (ASA)
Fig. 3 presents the evolution of the number of active sites which is directly related to the amount of carbonyl groups chemisorbed on the fibre after degassing at 950 °C. Active sites increase with the surface treatment but start to decrease slowly after 50% STL. The active surface area is obtained from these values (Table I) and the results show that surface treatment induces important changes in the chemical state of the fibre surface, but changes are not proportional to the level of surface treatment all the way up to the level of the commercial treatment.

3.4. X-ray photoelectron spectroscopy (XPS)
The oxidizing surface treatment clearly rendered the surfaces of the fibres more active and oxygenated groups have most probably been formed on active sites. As oxygen containing functionalities, the most referred groups in literature are alcohols, carbonyls, carboxylic acids and quinones [13–15]. Overall XPS spectra are not shown for any of the samples; they are
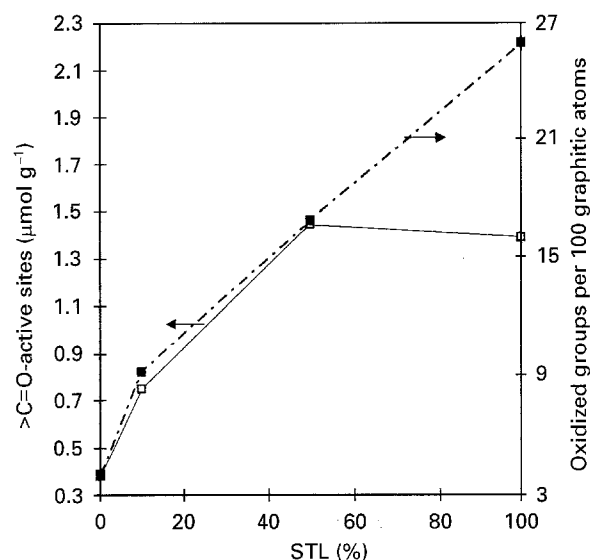

Figure 1 SEM image of an IM fibre.

Figure 3 Active surface area (in $>C=O$ $\mu moles^{-1} g$) as a function of STL obtained by ($\square$) chemisorption experiments, for comparison purposes, ($\blacksquare$) XPS results for oxygen containing groups, (in number of groups per 100 graphitic atoms at surface) are displayed.

TABLE I Active sites and active surface area of the fibres

STL (%)	Active sites (μmol $O_2 g^{-1}$)	Active area (ASA) ($cm^2 g^{-1}$)	ASA/BET (%)
0	0.38	380	3.2
10	0.75	750	6.3
50	1.44	1440	17.1
100	1.38	1380	18.4

all similar showing a strong C 1s peak, an O 1s peak and a very weak N 1s signal. The most widely suggested nitrogen containing groups are amines, amides and cyclic structures pyridine and piperidine type [16–20] and would originate from the residual nitrogen from PAN. All spectra were run in identical conditions taking into account a statistical improvement of the N 1s region. The values obtained in Lab 1 are plotted in Fig. 4 and clearly show the significant influence of STL on the surface composition, the contents of oxygen and nitrogen increasing regularly. These results were confirmed by the experiments in Lab 2 and Lab 3. All the results (in at %) are summarized in Table II; the small dispersion observed may arise from the fact that the analysed samples came from different points of the total length of treated fibre, since the electrical bath may slightly vary in its composition during the entire treatment.

To assess the amount of each particular chemical group introduced by the surface treatment, curve fitting of the C 1s, O 1s and N 1s peaks was performed. Controversies exist concerning this method and the validity of its results. The application of this method requires making choices about the characteristics of the peaks (the binding energies and chemical shifts assigned to each peak, the full width at half maximum, the shape of the peaks and the type of background). The fact that no universal procedure is followed for the choice of these parameters explains the controversial results found in literature, concerning carbon fibres. This problem has been studied by the authors
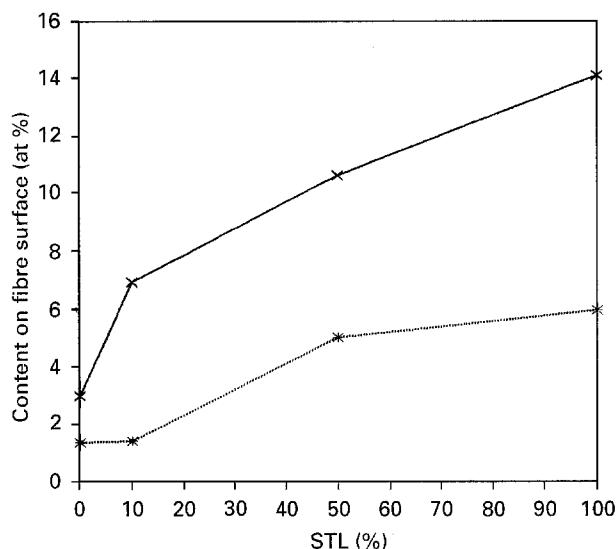

Figure 4 Amounts of ($\times$) oxygen and ($*$) nitrogen (in at %) on the fibre surfaces as a function of STL.

TABLE II Comparison of global amounts in at % of carbon, oxygen and nitrogen obtained in three different spectrometers

		0% STL	10% STL	50% STL	100% STL
	Lab 1	95.7	91.7	84.4	80.0
Carbon	Lab 2	94.2	90.6	85.2	80.2
	Lab 3	97.1	93.9	84.3	84.5
	Lab 1	3.0	6.9	10.6	14.1
Oxygen	Lab 2	4.2	7.5	9.3	13.3
	Lab 3	2.0	5.0	10.9	11.4
	Lab 1	1.4	1.4	5.0	5.9
Nitrogen	Lab 2	1.5	1.7	5.4	6.1
	Lab 3	0.8	1.0	4.8	4.1

and it has been decided that, in the choice of values for the curve fitting parameters, priority was given to internal consistency. By internal consistency we mean that the amount of oxygenated and nitrogenated functional groups found by curve fitting of C 1s peak must equal the sum of % O 1s and N 1s peaks. This is a concept increasingly considered by researchers as being logical from a chemical point of view [21].

With this priority in mind, all the C 1s spectra were curve-fitted with six peaks, the O 1s peaks with four peaks and the N 1s peaks with three peaks. The best internal consistency was obtained in the following conditions: curve fitting carried out with a nonlinear least-squares algorithm using a GL85 profile for all peaks and a Shirley background; binding energies of C 1s, O 1s and N 1s component peaks are given in Tables III, IV and V. The analysis was performed under a take-off-angle (TOA) of 90°.

The 0% fibre exhibits a mainly graphitic peak (284.4 eV) and a $\pi \rightarrow \pi^*$ transition at 290.2 eV. Fig. 5 shows C 1s peak for 0% and 100% STL fibre and for highly oriented pyrolytic graphite (HOPG). The graphitic structure almost disappears in the 10% STL fibre; simultaneously, the oxidized components and the aliphatic one (285.0 eV) increase, the C 1s peak becoming wider. This behaviour is enhanced in the

TABLE III Binding energies and assignment of the components of the C 1s peak and molar percentages of the oxidized ones (for 100% fibre) for all the analysed fibres
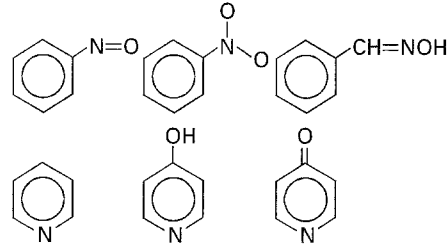
	BE(eV)	Functional groups	Molar % 0%	10%	50%	100%
C_1	284.4 ± 0.1	graphitic carbon				
C_2	285.0 ± 0.1	"aliphatic" carbon				
C_3	286.0 ± 0.1	("alcohol" group) COH; COC; CNH_2; > NH; [structures shown]	0.77	1.38	2.33	3.19
C_4	287.1 ± 0.1	("carbonyl" group) –C=N; >C=N-H; C=O; $CONH_2$; CNH_2COOH	1.52	1.82	5.17	5.62
C_5	288.5 ± 0.1	(carboxylic group) COOH; COOC	1.21	2.59	4.12	5.25
C_6	290.1 ± 0.3	$\pi \to \pi^*$ transition				

TABLE IV Assignment and mol% (for 100% fibre) of the components of the O 1s peak for all the analysed fibres

Carbon fibre STL (%)	O_1 (C=O) BE(eV)	(%)	O_2 (COOH) BE(eV)	(%)	O_3 (COH) BE(eV)	(%)	O_4 (COOH) BE(eV)	(%)
0	530.9	0.10	531.6	0.91	532.2	1.04	533.3	0.94
10	530.6	0.64	531.6	2.45	532.2	1.30	533.3	2.46
50	530.9	0.86	531.5	4.11	532.2	1.55	533.2	4.10
100	530.7	0.91	531.6	5.59	532.3	2.01	533.2	5.52

TABLE V Percentages and binding energies for the components of the N 1s peak (for 100% fibre) for all the analysed fibres

Carbon fibre STL (%)	N_1 BE(eV)	(%)	N_2 BE(eV)	(%)	N_3 BE(eV)	(%)
0	–	–	399.6	0.69	401.0	0.55
10	398.5	0.15	399.7	0.96	401.0	0.24
50	398.7	0.92	399.8	3.04	401.0	1.05
100	398.7	0.82	399.8	3.65	401.1	1.39

Figure 5 C1s peak for IM fibres compared with highly oriented pyrolitic graphite (HOPG): (a) 100% STL fibre; (b) 0% STL fibre; (c) HOPG. In the insert, an expansion of the $\pi \to \pi^*$ transition region, renormalized to the same base-line, is shown.

50% and 100% STL fibres where we can fit three oxidized components in the range 285.5–289 eV.

Fig. 6 displays the behaviour of carbon components found by curve fitting of C 1s peak, as a function of STL. The results presented in Table III and Fig. 6 reflect: (1) A degraphitization beyond the 10% STL; (2) An accentuated increase of the more oxidized groups – carboxylic group (BE = 288.5 ± 0.1) – with STL; (3) The presence of two types of carbon having intermediate binding energies, BE = 286.0 ± 0.1 and BE = 287.1 ± 0.1, assignable, respectively, to "alcohol" and "carbonyl" groups.

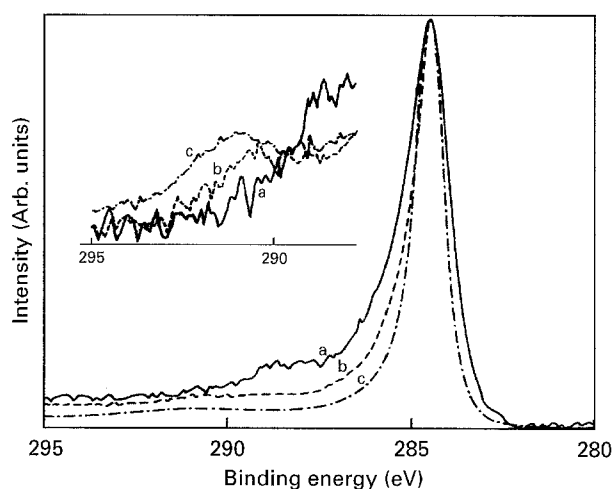Based on data from NIST Standard Reference Database [22] and recent literature [23], all the O 1s peaks were curve fitted with four peaks, assuming the assignment contained in Table IV. The results obtained with this assumption confirm the preferential formation of the carboxyl group by the STL.

The N 1s signal from the carbon fibres surface is much weaker than the C 1s or O 1s signals; therefore, a longer time of acquisition was used. The best
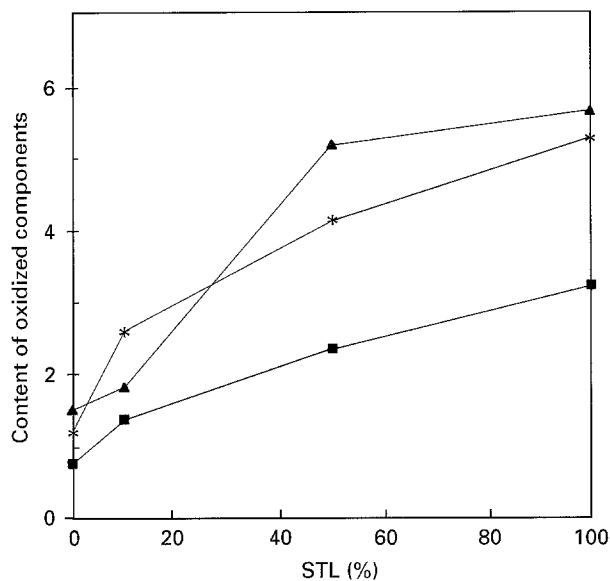
Figure 6 Percentages of "oxidized" components of the C1s peak, referred to 100% of fibre as a function of STL. Key: (■) C_3, (▲) C_4 and (*) C_5.

curve fitting was achieved with three peaks (BE = 398.5 ± 0.2, 399.7 ± 0.3 and 401.0 ± 0.3 eV) for 10%, 50% and 100% STL fibres. For the 0% STL fibre a new peak (BE = 402.6 eV) instead of the lowest BE one (BE = 398.5) was necessary to have a good curve fitting (Table V).

A tentative assignment of the N 1s peak components is as follows: in the surface treated fibres, the lowest BE peak may arise from aromatic amines and piperidine structures. The two higher BE peaks arise from residual nitrogen (aliphatic amines, nitrile, amides, amino-acids, cyclic structures – pyridine type – having oxygenated substituent groups). The peak at 402.6 eV can be assigned to highly oxidized nitrogen compounds (nitroso and nitro compounds).

The existence of the peak at 402.6 eV, in the 0% STL fibre (and absent in the other fibres), combined with the fact that the N 1s peaks are similar in the 50% and 100% STL fibres (both qualitatively and quantitatively) and qualitatively similar to the one in the 10% STL, is compatible with the following hypothesis: The surface treatment breaks down superficial "fringes" where nitrogen exists mainly un-incorporated in cyclic structures and at a lower density than in the bulk. Therefore, for larger STL most of the detected nitrogen is residual nitrogen from PAN remaining in the bulk and therefore exhibiting a similar distribution in all treated fibres where the destruction of the "fringes" is complete. This being the case, nitrogen would appear incorporated in saturated or unsaturated cycles for higher STL.

In the untreated fibre the "fringes" were not yet destroyed. For this reason the amount of nitrogen present at the surface is lower than in the highly treated surfaces and a small amount can be assigned to highly oxidized nitrogen compounds resulting from the carbon fibre production process itself. A similar assumption has already been reported by other authors [19, 24].

The hypothesis of nitrogen being put in the surface by the oxidative bath has been ruled out by running XPS spectra at several take-off angles: results show a decreasing nitrogen content from the bulk towards the surface [25]. Furthermore, over one of the fibres, the 100% STL, repeated spectra were run after being water boiled for 30 min and air dried at 130 °C and kept under UHV for 2 months. No qualitative or quantitative changes in the nitrogen, oxygen and carbon peaks have been noticed. Another spectrum was run after heating the same fibre, under UHV, to 250 °C for 30 min and, once more, no modifications have been noticed: namely the amount and the quality of nitrogen remained unchanged which would not happen if it was due to the oxidative bath.

As previously explained, the driving force in the curve fitting work has been the respect of internal consistency. This consistency has been obtained with a set of parameters which are in good agreement with values found in the literature. Global and partial consistency have been attained. The first one concerns the balance between the amount of functional groups obtained from the surface elemental composition and the curve fitting of C 1s, O 1s, and N 1s peaks. Indeed, taking into account that some carbon is bound to oxygen and to nitrogen, the O 1s% + N 1s% should be equal to the "oxidized" carbon% ($C_3 + C_4 + 2C_5$).

The multiplying factor for C_5 arises from the stoichiometry in carboxylic acids (O:C = 2:1). Other stoichiometries could be assumed namely for ethers (the BE coincides with the one for alcohols both for carbon and oxygen), esters, cyclic structures where the oxygen and the nitrogen are incorporated in the cycle, and compounds where the oxygen is directly bound to nitrogen (oximes, for instance).

The partial consistency, functionality by functionality, ($O_2 = O_4 = C_5$, $O_1 + N_1 + N_2 = C_3$, $O_3 + N_3 = C_4$) has been verified and the results are presented in Fig. 7.
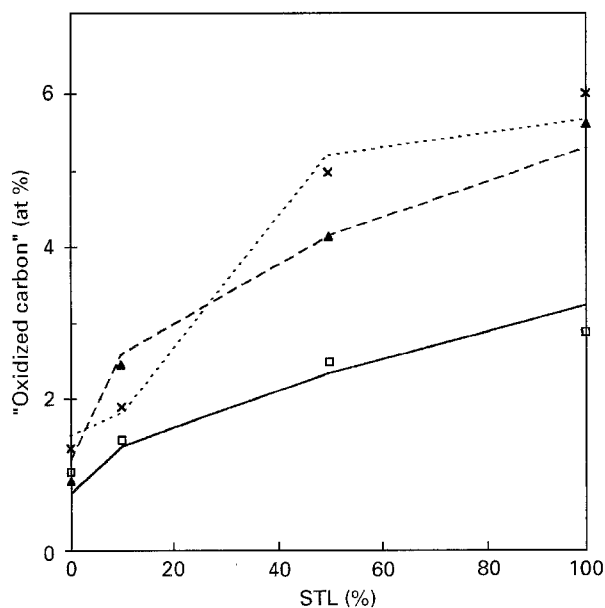

Figure 7 Verification of internal consistency of the XPS results. Key: (—) C_3 (C1s), (– –) C_4 (C1s), (- -) C_5 (C1s), (□) "C_3" (N1s + O1s), (×) "C_4" (N1s + O1s) and (▲) "C_5" (N1s + O1s).

Since the internal consistency reached with our assumption is remarkably good, it means that either the amount of other compounds where the stoichiometry is not 1:1 is negligible or there is a balance between the amount of compounds with multiplying factors greater than 1 and less than 1.

3.5. Surface energy properties

The surface energy and its polar and dispersive components vary with STL as is shown in Fig. 8. We can observe that STL increases mainly the polar component. This is associated with the development of polar functional groups, particularly oxygen containing, at the edge of graphitic basal planes.

3.6. Acid-base character of the fibres

The assessment of carbon-surface acidity or basicity can only be made tentatively from XPS data. According to Chan et al. [2], the surfaces of carbon fibres can be compared in terms of their relative acidity or basicity by measuring their contact angles using a given pair of probe liquids. In this case ethylene glycol and formamide were used as base and acid probes, respectively.

The acid-base surface interaction terms, γ_{SL}^{ab}, can be found, using the two liquids, according to the following formula [2]:

$$\gamma_{SL}^{ab(+,-)} = (1 + \cos\theta)\gamma_L - 2(\gamma_S^{LW}\gamma_L^{LW})^{0.5} \quad (1)$$

where γ_S^{LW} and γ_L^{LW} are, respectively, the dispersive components of the surface energy of the solid and the liquid, γ_L is the surface energy of the probe liquid and θ is the contact angle between the fibre and the liquid; the superscript $ab+$ denotes the acid character and the superscript $ab-$ denotes the basic character.

The results obtained are presented in Table VI and show the relative acid and base character of the 0% and 100% STL fibres. Both fibres are predominantly acid, which is in agreement with XPS observation from the curve fitting of the O 1s peaks. Moreover, the
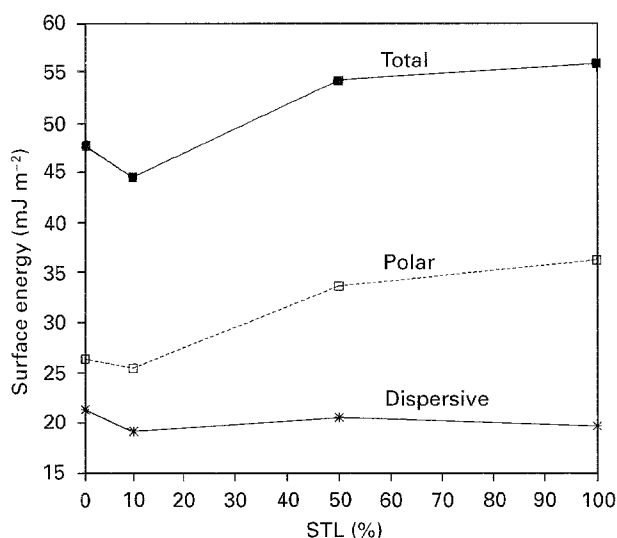
TABLE VI Acid–base properties of the fibre surface $(mJ\,m^{-2})$

Carbon fibre STL (%)	γ^{ab+}	γ^{ab-}	$\gamma^{ab+}/\gamma^{ab-}$
0	70.9	55.6	1.27
100	74.9	59.5	1.26

ratio of the acid and base components is nearly the same for both fibres, a conclusion that could not be derived from XPS results. In fact, neither by considering that all the C=O and the C–OH are totally basic or acidic nor by trying to weigh the acid and base character of both groups, could the ratio of 1.26 be obtained for both fibres. The possible presence of other groups besides the monitored oxygenated groups (COOH, C–OH and C=O), contributing to the acid–base character, and the presence of some carboxylic groups under the form of esters can explain this difference.

3.7. Correlations between the results of the fibre surface characterization

Some correlations between the obtained results may be established in order to propose a general view of the changes induced by the surface treatment on the surface of the IM fibres.

For instance, to correlate the active surface area measured by oxygen chemisorption (ASA) with the information on the chemical groups, as derived from XPS results, the specificity of the two techniques must be considered. Both allow the determination of the amount of sites which have been influenced by the surface treatment. The ASA technique seems to be more sensitive to the outermost layer; the XPS technique (TOA = 90°) measures the characteristics of a certain thickness of the material (typically 4 nm depending on the density of the material and on the escape depth of photoelectrons used in the analysis); however an angular analysis allows an estimation of the outermost layer characteristics. Anyway, by XPS, surface atomic percentages of oxygen (which, in principle, is introduced on active sites) are estimated whereas, by ASA, a number of active surface sites by unity of bulk material mass is measured. To make this last number comparable to XPS results, an estimation of the total number of atoms at the surface for the same amount of bulk material is then needed. The comparable values would then be on one hand the XPS fraction of oxygen at the outermost layer and, on the other hand, the ratio (number of active centres at the surface per gram)/(total number of atomic sites at the surface per gram).

By angular analysis, we have shown that the oxygen percentage at the outermost layer is about 30% larger than the average percentage measured at a TOA equal to 90° [25]. Then, we will multiply values in Table II by a factor of 1.3 to obtain the XPS percentage of oxygen at the outermost layer $((O\ XPS\%)_{surf})$.

The total number of atomic sites can be estimated from gas–solid adsorption isotherms assuming a BET model. The most used gas is the molecular nitrogen

Figure 8 Surface energy and its polar and dispersive components as function of STL.

whose generally accepted cross-sectional area is 0.162 nm^2; this corresponds approximately to the area occupied by 6 carbon atoms at the basal planes of graphite. However there is some evidence that, due to some constraints imposed by the geometrical parameters of the basal planes, the packing of the nitrogen molecules cannot be as dense as usual, bringing out a higher value for the cross-sectional area of the nitrogen molecule (about 0.2 nm^2) [26]. This last value corresponds to a ratio of 1:8 between the number of adsorbed nitrogen molecules and the number of carbon atoms at the surface. However, if the basal planes are perpendicular instead of parallel to the adsorbing surface, the geometrical constraints are smaller leading probably to the usual cross-sectional area of 0.162 nm^2. On the other hand, as the atomic density of these planes decreases (about 2:1), the number of carbon atoms corresponding to each nitrogen molecule will be approximately 3. Moreover, if we assume that graphite is not crystalline, presenting a lower density, we may expect ratios lower than 3 because the lower density is mostly due to a larger spacing between basal planes.

If we denote by n the number of sites at the fibre surface, per N_2 molecule, the number of sites per gram of fibre, n_f is:

$$n_f = n_{N_2} \times n \qquad (2)$$

where n_{N_2} is the number of moles of N_2 per gram of fibre obtained by BET.

The number of moles of active sites per gram of fibre, n_{as}, determined by ASA when multiplied by n_O, the number of oxygen atoms per active site, gives the number of moles of oxygen at the outermost layer by gram of fibre; n_O may be equal to unity for functionalities like carbonyl and alcohol but may be two for functionalities like esters or carboxylic acids; taking into account the curve fitting of oxygen peak in Table IV, we can estimate these numbers, for all the fibres, which are contained in Table VII:

$$n_O = \frac{O\%}{CO\% + COH\% + COOH\%} \qquad (3)$$

where all the percentages have been computed from XPS and are presented in Table II (the O percentage) and Table IV (the group percentages).

The oxygen percentage calculated from ASA/BET results is, then:

$$(O(ASA/BET)\%)_{surf} = \frac{n_{as} n_O}{n_{N_2} n} \times 100 \qquad (4)$$

By assuming that the percentage of oxygen at the outermost fibre surface calculated from the ASA/BET

and the XPS results is the same:

$$(O(ASA/BET)\%)_{surf} = (O(XPS)\%)_{surf}$$

we can compute the number n that makes XPS and ASA/BET results to match, i.e.:

$$n = \frac{100 \; n_{as} n_O}{(O \; XPS\%)_{surf} \; n_{N_2}} \qquad (5)$$

Table VII presents XPS, ASA and adsorption results as well as the values of the number n:

If we admit that all the experimental results are known with an error $\leqslant 5\%$, then n can be estimated with an accuracy better than 15%. So, the evolution of the relative values of n is meaningful and this would indicate a non-monotonic effect of the treatment level over the fibre density at the surface. The obtained values for n show that the fibre surface is far from being formed by graphitic basal planes. However they are larger than they would be in a non crystalline graphitic structure with the basal planes perpendicular to the adsorbing surface. The 10% STL fibre is an exception, the low value of n denoting a destructive process induced by this level of treatment on the fibre surface.

This correlates with the STM results showing the attack of the surface treatment on the 10% fibre (low n value). Further treatment reveals two zones: one with graphitic basal planes and another one with a row of interleaved blocks with large plane surfaces and smaller perpendicular faces (high n values). When the treatment is extended to 100%, pits are introduced on the large plane surfaces inducing a decrease of the n value. Therefore, we have shown that not only ASA/BET and XPS results can be correlated but also that such correlation can provide more information about the outermost layer structure.

Another correlation that can be done is between ASA and STM results. Indeed ASA results agree with STM conclusions drawn by Marshall and Price [12], for the 50 and 100% STL treated IM fibres: the presence of two regions at the fibre surface, one of which containing steps. In fact, as is often reported in literature [27], most of the functional groups are placed at the edges of the basal planes. From the results of Marshall and Price [12] and Desaeger's interpretation [28], one half of the fibre surface presents no edge sites and, in the step region, the steps occupy 50% of the specific area of this region. Therefore, assuming a total surface area of 1 $m^2 g^{-1}$, the percentage of edge surface was calculated to be 25%.

ASA measurements led to a percentage of active surface area of approximately 10%. So, the hypothesis

TABLE VII Correlation between XPS and ASA results

Carbon fibre STL (%)	Active sites $\times 10^{-6} \; n_{as}$ (moles g^{-1})	n_O	Adsorbed N_2, $\times 10^{-5} \; n_{N_2}$ (moles g^{-1})	Oxygen (XPS%)$_{surf}$	n
0	0.76	1.46	1.14	3.9	3.24
10	1.50	1.56	1.21	9.0	2.80
50	2.88	1.62	0.887	13.8	4.99
100	2.76	1.65	0.777	18.3	4.17

that the functional groups at the outermost layer of fibre surface are placed on the edges of the basal planes is possible, the edge surface being large enough (25%) to be occupied by the active sites (10%).

The XPS results also agree qualitatively with the data obtained by the contact angle method used to establish the general acid–base properties of the fibres. The usually adapted acid and base probes have shown that the outermost layer of the fibre surface is, in the case of the 0 and 100% STL fibres, predominantly acidic. The carboxylic acid groups, the presence of which has also been confirmed with the XPS measurements, are strong acid groups. Therefore, even if other components contribute to the acid and basic character of the fibre, the larger part of the acidic character is probably induced by the strong acidic carboxylic acid groups.

3.8. General view of the fibre surface

The complementary use of the surface characterization techniques has allowed us to derive a general scheme of the fibre surface (Fig. 9): Carbon "fringes", detected by STM and XPS, are present on the surface of 0% STL fibre. These fringes are destroyed by the surface treatment; which, first renders some sites ac-
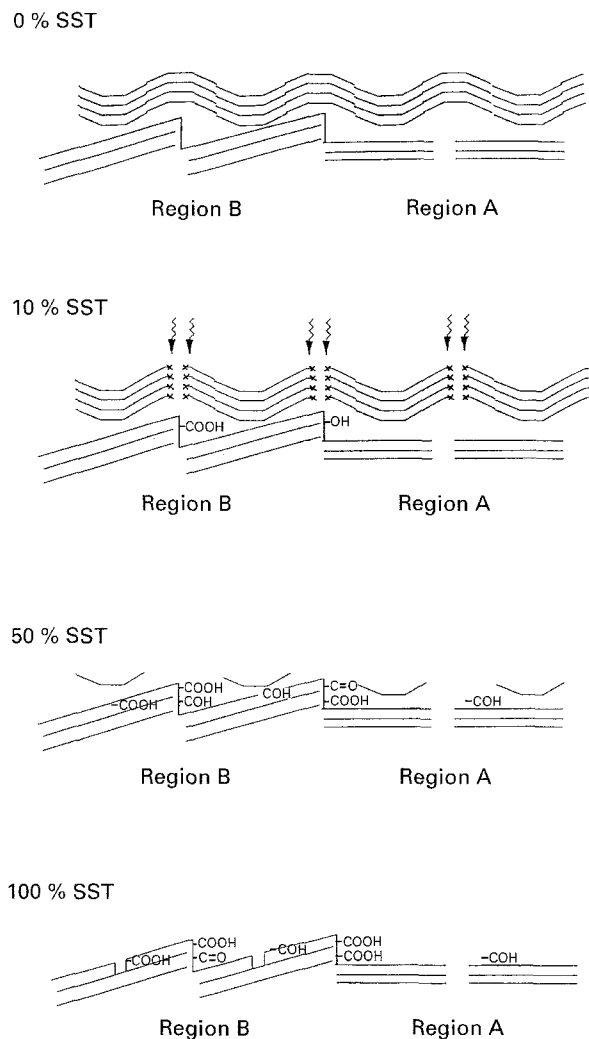

Figure 9 General overview of the effect of the surface treatment on the fibre surface.

tive and, then, introduces oxygen onto these sites. The start of the surface treatment introduces inhomogeneity at the fibre surface (attested to by the large standard deviation on the 10% STL results and the low value of n for that same fibre) but when conducted to a larger extent, reveals two regions of different structure (STM [12]). At the same time, the amount of oxygen placed at the fibre surface, increases and is mostly converted into carboxyl groups (XPS, Table II) even if the acid/base ratio stays the same (contact angle measurements, Table VI). The specific surface area decreases (Fig. 2), even if locally the structure changes. When conducted to a large extent (100% STL) the treatment introduces pits on the basal planes (STM [12]) which ensures also a decrease of the n value.

3.9. Correlations with interface micromechanical properties

The use of micromechanical test techniques (microindentation, fragmentation and pull-out tests) has shown interesting facts [28]. These techniques allow the direct determination of the interface properties which are greatly influenced by the state of the fibre surface. The appropriate use of these tests allows the separate determination of the interfacial bond shear and the interfacial frictional resistance, which can be correlated to the state of the fibre surface. The results of these tests are the scope of references [28, 29] and can be summarized as follows:

(i) The interfacial bond shear strength (i.e., the critical stress for rupture in shear of the links between the fibre and the matrix) is mostly influenced by the local morphology of the outermost graphitic surface layers and by the number of active sites. These facts contribute 85% to the interfacial bond shear strength in the case of the studied carbon fibres embedded in an epoxy matrix. The remaining 15% is due to the presence of oxygen introduced by the treatment, which has generated active centres.

(ii) The interfacial frictional resistance (i.e., the load transfer capability which exists when two broken parts of the interface region are still in contact) is mostly influenced by the global surface area and local configuration of the carbon planes of the fibre surface.

It is interesting to note that the results found about the factor n confirm the previous finding concerning the interfacial frictional resistance. The variation of this factor with the surface treatment is the inverse of the variation of the frictional resistance [28, 29]. In Fig. 10 the correlation is shown. This supports the idea of a large contribution of the interlocking mechanism to the frictional resistance between the fibre and the matrix since a denser surface (i.e., a surface with graphitic planes lying parallel to the fibre surface) diminishes the friction and a lower atomic density at the surface (*inter alia* due to the presence of graphitic planes perpendicular to the surface) increases it.
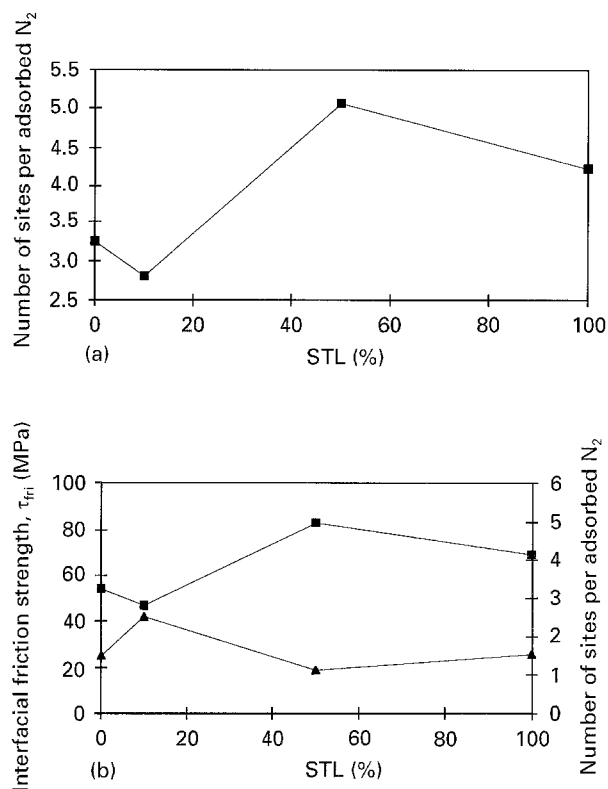
Figure 10 (a) Number of sites per adsorbed N_2 molecule at the fibre surface, n, resulting from the combined results of XPS and BET/ASA, as a function of percentage of STL. (b) Correlation between the interfacial friction strength τ_{fri} (▲) and n (■).

4. Conclusions

The surface characterization of the IM 43-750 surface treated fibres, through the use of a large number of experimental techniques and some recent results from literature, provided a general picture of the state of each carbon fibre. In summary, the application of different degrees of surface treatment mainly induces:

(i) A decrease of the global fibre surface area after a small increase for the 10% STL fibres. The latter fibres also showed the largest microporosity.

(ii) A destruction of the outermost surface layer leading to a configuration and chemical composition different from the graphitic layers found closer to the centre of the fibre.

(iii) The display of local microrelief made out of steps protruding from the fibre surface. This microrelief appears after the destruction of the outermost graphitic layer and is obtained for a treatment level equal to or higher than 50%. The steps become pitted for a treatment higher than 50%.

(iv) The activation of the fibre surface. Carbon atoms which were inactive before the surface treatment become activated; this means an easy reaction with oxygen to form oxygenated complexes.

(v) The introduction of oxygenated groups which are, amongst others, in the form of COOH, COH and C=O, the COOH groups being the predominant ones.

(vi) The increase of surface energy, basically due to an increase in the polar component; this fact is compatible with the increase in carboxylic and nitrogen containing groups.

The results have allowed us to outline important surface features which can improve the adhesion between the fibre and an epoxy matrix. Micromechanical tests (microindentation, pull-out and fragmentation) were performed [28] for the evaluation of the interphase properties, showing the following relationships:

(i) The interfacial bond shear strength seems to be predominantly influenced by the presence of active sites at the fibre surface and the microrelief.

(ii) The improvement of the bond shear strength is also, at least, to a certain extent, influenced by the amount of the oxygen present on the active sites of the fibre surface. Nevertheless, the contribution of the total amount of oxygen seems to be less important than the contribution of the total number of active sites.

(iii) The interfacial frictional resistance seems to be influenced by the global topography of the fibre surface. The load transfer by friction is enhanced in fibres having a large global surface area. Nevertheless, the interfacial frictional resistance is also influenced by local effects and the configuration of the carbon planes.

References

1. C. F. HOLLEYMAN, in "Carbon Fibres, Technology, Users and Prospects," (Plastics and Rubber Institute, London, 1986) p. 29.
2. D. CHAN, M. A. HOZBOR, E. BAYRAMLI and R. L. POWELL, *Carbon* 29 (1991) 1091.
3. D. W. McKEE and V. J. MIMEAULT, in: "Chemistry and Physics of Carbon," Vol. 8, edited by P. L. Walker, Jr. and P. A. Thrower (Marcel Dekker, New York, 1973) p. 151.
4. M. DESAEGER and I. VERPOEST, in "Interfaces in New Materials," edited by P. Grange and B. Delmon, (Elsevier, Amsterdam, 1990) p. 95.
5. B. RAND and R. ROBINSON, *Carbon* 15 (1977) 2547.
6. C. KOZLOWSKI and P. M. A. SHERWOOD, *ibid.* 25 (1987) 751.
7. Y. XIE and P. M. A. SHERWOOD, *Chemistry of Materials* 1 (1989) 427 and references therein.
8. T. TAKAHAGI and A. ISHITANI, *Carbon* 26 (1988) 389.
9. P. DENISON, F. R. JONES and J. F. WATTS, *J. Phys. D: Appl. Phys.* 20 (1987) 306.
10. D. H. KAELBLE, P. J. DYNES and E. H. CIRLIN, *J. Adhesion* 6 (1974) 23.
11. J. B. DONNET and H. DAUKSCH, Proceedings of the International Carbon Fibres Conference, London, 1971 (The Plastics Institute, London 1971) 49.
12. P. MARSHALL and J. PRICE, *Composites* 22 (1991) 388.

13. D. M. BREWIS, J. COMYN, J. R. FOWLER, D. BRIGGS and V. A. GIBSON, *Fibre Sci. Technol.* **12** (1979) 41.
14. K. WALTERSSON, *ibid.* **17** (1982) 289.
15. Y. NAKAYAMA, F. SOEDA and A. ISHITANI, *Carbon* **28** (1990) 21.
16. C. KOZLOWSKI and P. M. A. SHERWOOD, *ibid.* **24** (1986) 357.
17. Y. XIE and P. M. A. SHERWOOD, *Applied Spectroscopy* **43** (1989) 1153.
18. C. JONES and E. SAMMAN, *Carbon* **28** (1990) 509.
19. C. JONES, *Surface Interface Analysis* **20** (1993) 357.
20. R. H. BRADLEY, X. LING, I. SUTHERLAND and G. BEAMSON, *Carbon* **32** (1994) 185.
21. E. DESIMONI, G. I. CASELLA, A. M. SALVI, T. CATALDI and A. MORONE, *ibid.* **30** (1992) 527.
22. C. D. WAGNER, "NIST X-ray Photoelectron Spectroscopy Database," (U.S. Dep. of Commerce, Washington D.C. 1989).
23. G. BEAMSON and D. BRIGGS, "The Scienta ESCA 300 Database", (John Wiley, Chichester, 1992).
24. K. MORITA, Y. MURATA, A. ISHITANI, K. MURAYAMA, T. ONO and A. NAKAJIMA, *Pure & Appl. Chem.* **58** (1986) 455.
25. M. J. REIS, A. M. BOTELHO do REGO, J. D. LOPES da SILVA and M. N. SOARES, *J. Mater. Sci.* **30** (1995) 118.
26. C. PIERCE and B. EWING, *J. Phys. Chem.* **68** (1964) 2562.
27. C. KOZLOWSKI and P. M. A. SHERWOOD, *J. Chem. Soc. Faraday Trans. I* **81** (1985) 2745.
28. M. DESAEGER, PhD thesis, Katholieke Universiteit Leuven, (1993).
29. T. LACROIX, R. KEUNINGS, M. DESAEGER and I. VERPOEST, *J. Mater. Sci.* **30** (1995) 683.